Int. J. Electrochem. Sci., 17 **(2022)** Article Number: 220450, doi: 10.20964/2022.04.52

International Journal of
ELECTROCHEMICAL
SCIENCE
www.electrochemsci.org

Short Communication

Corrosion Investigation of Self-cleaning Film Prepared on Surface of Hot-dip Galvanized Steel in Chloride-bisulphite Mixed Solution

Fa Wang, Yue Yao, Wei Han, Lankang Zhu[*]

Jiaxing Hengchuang Electric Power Design and Research Institute, Jiaxing 314033, China
E-mail: Institute_wang22@163.com

Received: 11 January 2022 / *Accepted:* 10 February 2022 / *Published:* 4 March 2022

A passivated hot-dip galvanized steel was prepared using passivation technology, and then a self-cleaning film was generated by spraying modified TiO_2 sol on the passivated hot-dip galvanized steel. The surface morphology and component of the film were characterized, and the surface wettability, self-cleaning performance and corrosion resistance of the film were tested and analyzed. The results show that the film is prepared by a modified TiO_2 sol attached to the surface of passivated hot-dip galvanized steel, which has a micro and nano rough structure resulting in a superhydrophobic surface (static contact angle is up to 151.4°). The film is more effective at preventing corrosive media from penetrating and reducing the adherence of liquid pollutants. Moreover, the film not only makes the surface of hot-dip galvanized steel not easy to be polluted, but also significantly improves the corrosion resistance of hot-dip galvanized steel, which has a splendid prospect application for transmission tower to prolong its service life.

Keywords: self-cleaning film; hot-dip galvanized steel; power transmission tower; surface wettability; self-cleaning performance; corrosion resistance

1. INTRODUCTION

The reliability of transmission line is related to the safe operation of transmission network. As an important infrastructure of power industry, power transmission tower supports transmission lines to make them layout according to the set path [1-6]. In terms of material, the power transmission tower generally uses hot-dip galvanized steel. This material not only has the excellent mechanical properties, but also shows good corrosion resistance. The galvanized layer plays a dual role of blocking corrosive media and sacrificing the anode [7-10]. However, after several years of use, the galvanized layer on the surface of hot-dip galvanized steel will be corroded to different degrees, resulting in a reduction in its protective function, and then affect the service life of power transmission tower. In order to further

improve the corrosion resistance of hot-dip galvanized steel, and to give it self-cleaning performance which is not easy to be polluted, it is necessary to carry out surface treatment for hop-dip galvanized steel.

At present, passivation is a common surface treatment method for hot-dip galvanized steel and some zinc alloys, which has the advantages of simple process, low cost and good corrosion resistance [11-16]. However, the self-cleaning performance of passivation film is not good enough. In addition, long-term exposure to corrosive media such as chloride ions will adversely affect the durability of passivation film. The surface coated with superhydrophobic and self-cleaning film is expected to better block corrosive media and pollutants [17-20]. Therefore, the surface of hot-dip galvanized steel with self-cleaning characteristics can significantly improve the corrosion and pollution resistance, so that the transmission tower is not easily polluted and ensure the service life to meet the requirements. In view of this, the paper uses the combination of passivation and spray treatment to prepare a passivation film on the surface of hot-dip galvanized steel firstly, and then sprays modified sol on the surface of passivation film to form a self-cleaning film.

2. EXPERIMENTAL

2.1 Materials

HDGS as acronym for hot-dip galvanized steel (coating thickness is about 20 μm) was used as the substrate, and the samples were cut to meet the requirements of the experiment. After oil removal (acetone, ultrasonic cleaning for 5 min), pickling (hydrofluoric acid with volume fraction of 5%, soaking at room temperature for 1 min) and deionized water cleaning, the substrate is then placed in the air drying oven. The reagents used in the experiment are mainly cerium nitrate, hydrogen peroxide, TiO_2 sol (nano-TiO_2 particle content is about 30%), polydimethylsiloxane, curing agent and xylene. The entire purity grade is analytical pure.

2.2 Preparation of a self-cleaning film on HDGS

Figure 1 shows the process of preparing a self-cleaning film on HDGS, which is described as follows:

(1) The HDGS sample after treatment was immersed in cerium salt solution (22 g/L cerium nitrate, 15 mL/L hydrogen peroxide) and passivated for 30 min, then cleaned and dried with deionized water and blower to get the passivated HDGS.

(2) Polydimethylsiloxane and curing agent were mixed according to the mass ratio of 10:1, and after being evenly stirred, they were slowly added to the mixed solution of TiO_2 sol and xylene. The modified TiO_2 sol was prepared by continuous magnetic stirring for 2 h.

(3) The modified TiO_2 sol was uniformly sprayed onto the surface of the passivated HDGS with a spray gun, and then placed in a dry place at room temperature for curing. After curing, the modified TiO_2 sol was adhered to the surface of the sample to obtain a self-cleaning film on HDGS.

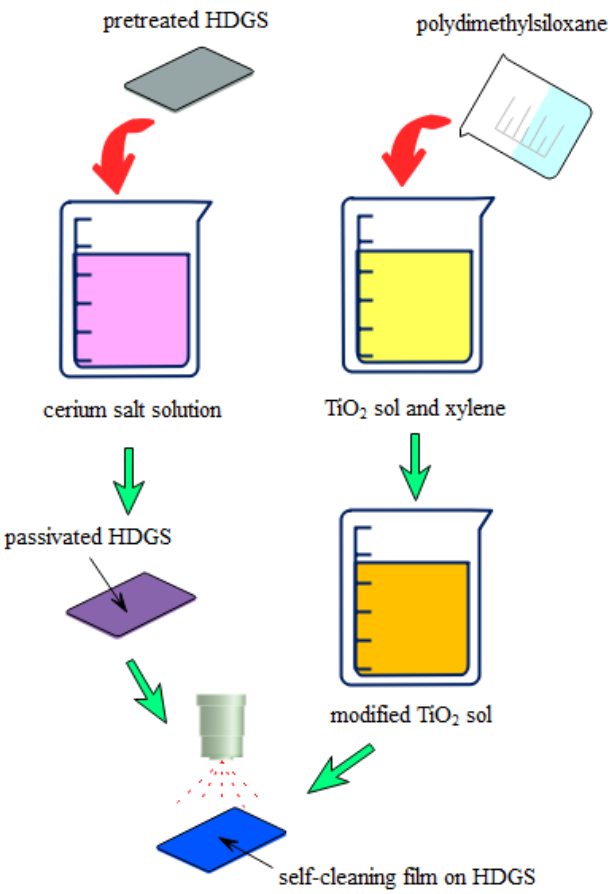

Figure 1. Process of preparing a self-cleaning film on HDGS

2.3 Characterization and performance test

2.3.1 Morphology characterization

The morphology of the film was characterized by SU-5000 scanning electron microscope, and the surface component of the film was analyzed by energy dispersive spectrometer.

2.3.2 Surface wettability and self-cleaning performance test

The static contact angle of the film was measured by XG-CAMA contact angle measuring instrument, and the surface wettability was evaluated. The volume of water droplet was controlled to be 4 μL, and the water droplet was placed at three different positions on the surface of the film. The measurement results were averaged to reduce the error.

Dust, soil and water are mixed according to a certain mass ratio to simulate liquid pollutants, and liquid pollutants are absorbed on the surface of the film with a syringe to observe the droplet morphology. At the same time, the sample was tilted at a certain angle to observe the droplet position and morphology changing to evaluate whether the film has self-cleaning performance.

2.3.3 Corrosion resistance test

PARSTAT 2273 electrochemical workstation was used to test the polarization curve and electrochemical impedance spectrum of the film in 0.05 mol/L sodium chloride and 0.01 mol/L sodium bisulfite mixed solution as the corrosion medium. The saturated calomel electrode and platinum electrode were used as the reference electrode and the assistant electrode, respectively. The test sample was as the working electrode. In the open-circuit potential test, the scanning rate of the polarization curve was 1 mV/s. In the electrochemical impedance spectroscopy test, the high frequency was 10^5 Hz and the low frequency was 10^{-2} Hz with 5 mV sine wave excitation signal. Tafel extrapolation method was used to fit the polarization curve test data to obtain the corrosion potential and corrosion current density. ZSimpWin software was used to fit the electrochemical impedance spectrum test data to obtain the charge transfer resistance and film resistance.

3. RESULT AND DISCUSSION

3.1 Surface morphology and component

Figure 2(a) shows the morphology of hot-dip galvanized steel. It can be seen that the surface of hot-dip galvanized steel is smooth. Figure 2(b) shows the morphology of passivated HDGS. It can be seen that many slender cracks are crisscrossed on the surface of passivated HDGS which is similar to the morphology reported by some investigators [21-24]. Figure 2(c) shows the morphology of the self-cleaning film on HDGS. It can be seen that a large number of nano level holes and micron level protrusions are formed on the surface of the self-cleaning film, presenting a micro and nano rough structure, which is the key factor for the superhydrophobic state of the film surface [25-27].

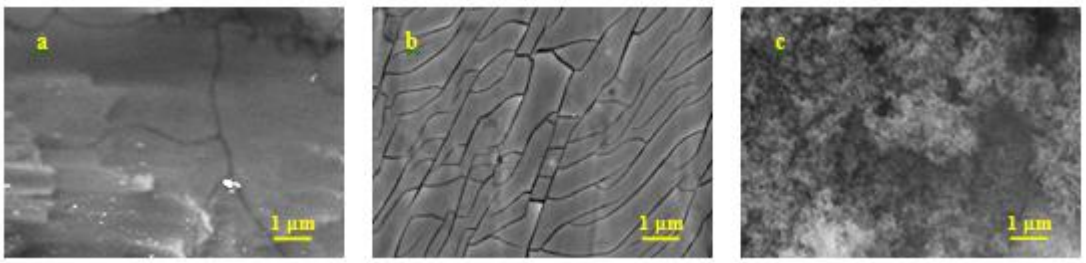

Figure 2. Morphology of different films on the surface of hot-dip galvanized steel; a-hot-dip galvanized steel; b-passivated HDGS; c-self-cleaning film on HDGS; (sample size 10 mm×10 mm×1 mm, acceleration voltage 15 kV, magnification 35000 times, automatic focus shooting)

Figure 3(a) shows the component analysis results of hot-dip galvanized steel, and Figure 3(b) shows the component analysis results of passivated HDGS. By comparing Figure 3(a) and Figure 3(b), it can be seen that the surface component of hot-dip galvanized steel changes significantly after passivation treatment, because a passivation film containing cerium is formed to cover the surface of hot-dip galvanized steel. Figure 3(c) shows the component analysis results of the self-cleaning film on

HDGS. Therefore, it can be inferred that the film is mainly composed of Ce, Ti, C and Si elements. The presence of Ti, C and Si elements indicates that TiO_2 particles participate in the film forming process combined with polydimethylsiloxane.

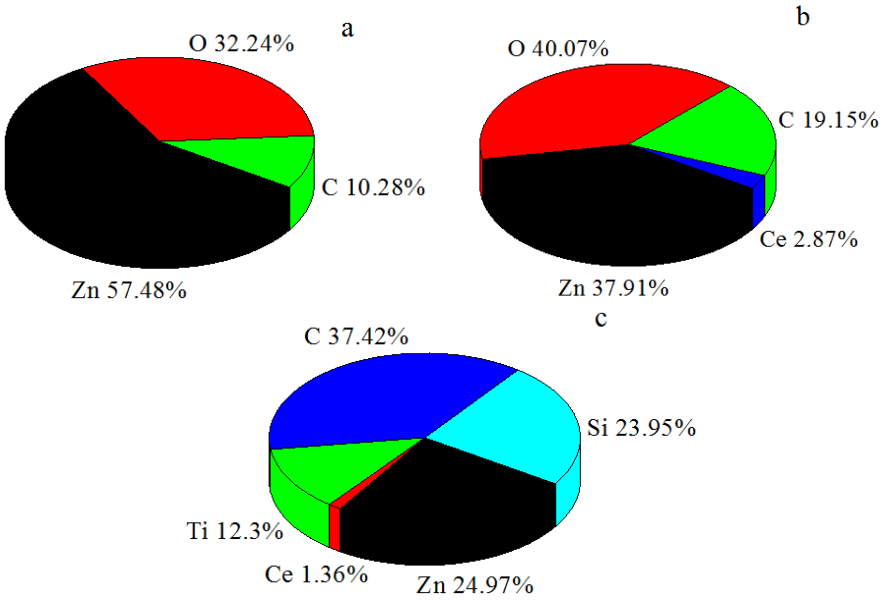

Figure 3. Component analysis results of different films on the surface of hot-dip galvanized steel; a-hot-dip galvanized steel; b-passivated HDGS; c-self-cleaning film on HDGS (surface sweep model, accelerating voltage 10 kV, sampling depth 1 μm)

3.2 Surface wettability

Table 1. Static contact angle of hot-dip galvanized steel and different films (volume of water droplet was 4 μL, magnification 5 times, automatic focus shooting, measurement accuracy 0.1°)

Samples	**Water droplet morphology**	**Static contact angle/ °**
hot-dip galvanized steel		73.6
passivated HDGS		102.7
self-cleaning film on HDGS		151.4

Table 1 lists static contact angles of hot-dip galvanized steel and different films. The static contact angle of hot-dip galvanized steel is 73.65° and its surface is hydrophilic. The static contact angle of the passivated HDGS increases to 102.7°, presenting a hydrophobic state. The static contact angle of the self-cleaning film reaches 151.4° and exceeds 150°, and the surface is superhydrophobic. This is because the film has a micro and nano rough structure that can capture air and form a gas film on its surface, which reduces the solid and liquid interface contact area and inhibits the spread of water droplets. The rough structure of materials with superhydrophobic performance is also investigated by some people [28-30]. In addition, the adhesion of polydimethylsiloxane after curing makes the film have low surface energy and weak affinity to water droplets, thus showing a superhydrophobic state.

3.3 Self-cleaning performance

Figure 4 shows the appearance of liquid pollutants falling on the surface of hot-dip galvanized steel and different films. It can be seen from Figure 4(a) and Figure 4(b) that the liquid pollutants on the surface of hot-dip galvanized steel and passivated HDGS tend to slip downward. The contaminated area is large, indicating that the surface of hot-dip galvanized steel and passivated HDGS is easy to be polluted. According to Figure 4(c), the liquid pollutants falling on the surface of the self-cleaning film are approximately spherical. The liquid pollutants can roll downward quickly to prevent pollution. This is because the film has a micro and nano rough structure with lower surface energy, presenting a superhydrophobic state. The liquid pollutants are difficult to stick to its surface, thus showing good self-cleaning performance and not easy to be polluted. The TiO_2 particles are also reported to be used to improve self-cleaning performance of materials [31-34].

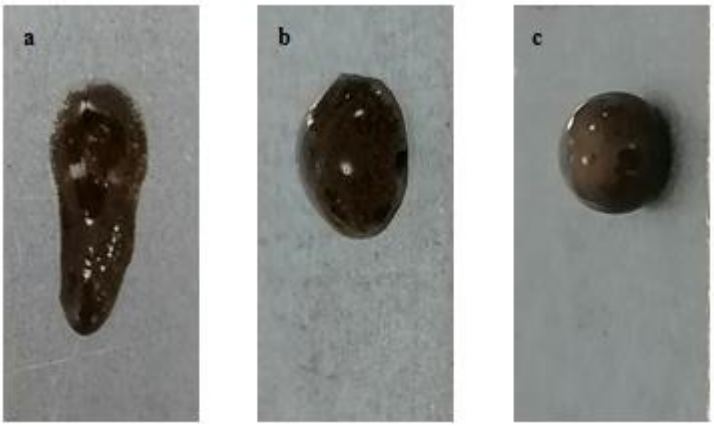

Figure 4 Morphology of liquid pollutant fall on the surface of hot-dip galvanized steel and different films; a-hot-dip galvanized steel; b-passivated HDGS; c-self-cleaning film on HDGS (dust, soil and water mixed solution as liquid pollutants, magnification 5 times, automatic focus shooting)

3.4 Corrosion resistance

Figure 5 shows the polarization curves of hot-dip galvanized steel and different films while Figure 6 shows the fitting results of polarization curves. Combined with Figure 5 and Figure 6, it can

be seen that the corrosion potential of the self-cleaning film is the most positive compared with that of hot-dip galvanized steel and passivated HDGS. The corrosion current density of the film is also the lowest, which is around 8 μA/cm^2. The changes of corrosion potential and current density indicate that the self-cleaning film has the best corrosion resistance and can effectively inhibit the electrochemical corrosion of hot-dip galvanized steel.

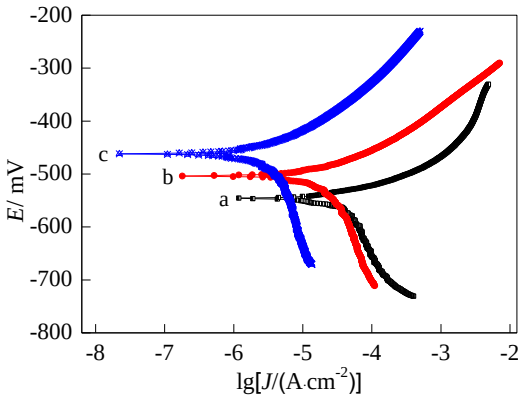

Figure 5. Polarization curves of hot-dip galvanized steel and different films; a-hot-dip galvanized steel; b-passivated HDGS; c-self-cleaning film on HDGS (corrosion medium was 0.05 mol/L sodium chloride + 0.01 mol/L sodium bisulfite, saturated calomel electrode as reference electrode, platinum electrode as assistant electrode and test sample as working electrode, scanning rate of polarization curve was 1 mV/s)

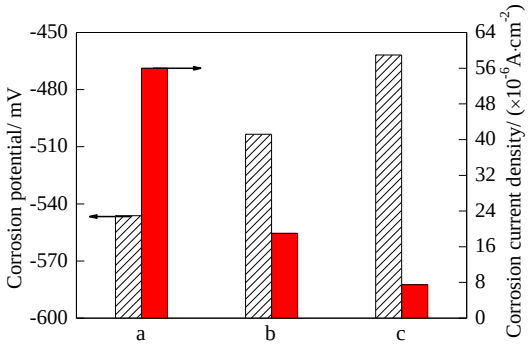

Figure 6. Polarization curves fitting results; a-hot-dip galvanized steel; b-passivated HDGS; c-self-cleaning film on HDGS

Figure 7 shows the electrochemical impedance spectra of hot-dip galvanized steel and different films. It can be seen that hot-dip galvanized steel, passivated HDGS and self-cleaning film on HDGS all show the characteristics of single capacitance-arc resistance. The order of capacitance-arc radius from large to small is self-cleaning film on HDGS, passivated HDGS and hot-dip galvanized steel. According to equivalent circuit fitting, charge transfer resistance and film resistance are obtained as shown in Figure 8, in which charge transfer resistance represents the difficulty of electron transfer between the film and the corroded medium. The film resistance can reflect the protective effect of the film's ability to resist the corroded medium. It can be seen from Figure 8 that the charge transfer resistance of the self-cleaning film is the highest, reaching 8107.5 Ω·cm^2, which is about 2 times

higher than that of hot-dip galvanized steel, indicating that the resistance of electron transfer between the film and the interface of the corrosive medium is greater, and the electrochemical corrosion process is suppressed to a certain extent. The film resistance of the self-cleaning film is also the highest, reaching 2026.8 $\Omega \cdot cm^2$. The ability of the film to resist corrosive media is stronger, and its protection effect on hot-dip galvanized steel is obviously better than that of passivated HDGS. The analysis shows that the film has a superhydrophobic state with micro and nano rough structure, which can better prevent the penetration of corrosive medium, resulting in good corrosion resistance. The superhydrophobic state is conducive to improving corrosion resistance of materials which is also studied in many works [35-37].

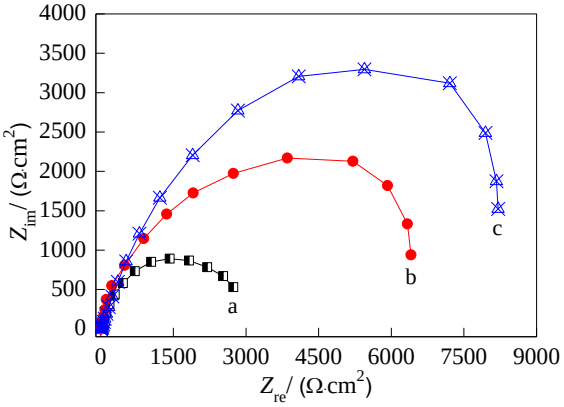

Figure 7. Electrochemical impedance spectrum of hot-dip galvanized steel and different films; a-hot-dip galvanized steel; b-passivated HDGS; c-self-cleaning film on HDGS (corrosion medium was 0.05 mol/L sodium chloride + 0.01 mol/L sodium bisulfite, saturated calomel electrode as reference electrode, platinum electrode as assistant electrode and test sample was as working electrode, scanning from high frequency 10^5 Hz to low frequency 10^{-2} Hz with 5 mV sine wave excitation signal)

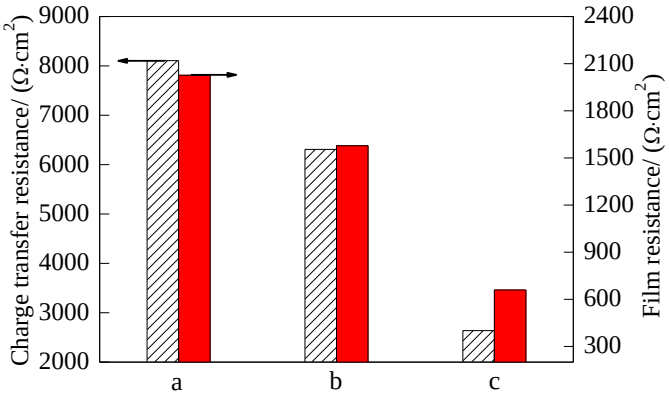

Figure 8. Electrochemical impedance spectrum fitting results; a-hot-dip galvanized steel; b-passivated HDGS; c-self-cleaning film on HDGS

4. CONCLUSIONS

Passivation and spray of modified TiO_2 sol treatment were combined to prepare a self-cleaning film on the surface of hot-dip galvanized steel. The surface of the film is superhydrophobic with static contact angle of 151.4°, which can effectively stop the corrosive medium permeability while also showing good self-cleaning performance and corrosion resistance. The film has a micro and nano rough structure and lower surface energy, which can capture air and form a gas film on the surface to effectively inhibit the corrosion process. Compare with hot-dip galvanized steel, the film has the most positive corrosion potential and the lowest corrosion current density with the largest charge transfer resistance which contribute directly to optimal corrosion resistance and self-cleaning performance.

ACKNOWLEDGEMENT
The study was supported by “State Grid Zhejiang Electric Power Co., Ltd. Technology Project 5211JY20001P”.

References

1. S. Gao, C. Zeng, L. Q. Zhou, X. H. Liu and B. Y. Gao, *Structures*, 24 (2020) 1.
2. A. A. Zekavati, M. A. Jafari and A. Saeedi, *Structures*, 35 (2022) 833.
3. J. Y. Xue, F. Mohammadi, X. Li, M. Sahraei-Ardakani, G. Ou and Z. X. Pu, *Reliab. Eng. Syst. Saf.*, 203 (2020) 107079.
4. Q. J. Shu, G. L. Yuan, Z. H. Huang and S. Ye, *Eng. Struct.*, 123 (2016) 166.
5. Y. Z. Cai, Q. Xie, S. T. Xue, L. Hu and A. Kareem, *Eng. Struct.*, 191 (2019) 686.
6. N. Lashmar, S. Y. Berryman, M. J. Liddell, A. L. Morrison, L. A. Cernusak, T. D. Northfield, S. Goosen and B. Jennison, *J. Environ. Manage.*, 252 (2019) 109430.
7. H. Kancharla, G. K. Mandal, S. S. Singh and K. Mondal, *Surf. Coat. Technol.*, 4 (2022) 128071.
8. P. A. Kamble, P. P. Deshpande and S. T. Vagge, *Mater. Today*, 13 (2021) 12.
9. A. Al-Negheimish, R. R. Hussain, A. Alhozaimy and D. D. N. Singh, *Constr. Build. Mater.*, 274 (2021) 121921.
10. D. Nakhaie, A. Kosari, J. M. C. Mol and E. Asselin, *Corros. Sci.*, 164 (2020) 108310.
11. Y. D. Yu, X. X. Zhao, M. G. Li, G. Y. Wei, L. X. Sun and Y. Fu, *Surf. Eng.*, 29 (2013) 743.
12. H. Yang, X. H. Kong, W. H. Lu, Y. X. Liu, J. Guo and S. S. Liu, *Prog. Org. Coat.*, 67 (2010) 375.
13. C. Y. Tsai, J. S. Liu, P. L. Chen and C. S. Lin, *Surf. Coat. Technol.*, 205 (2011) 5124.
14. F. Tittarelli and T. Bellezze, *Corros. Sci.*, 52 (2010) 978.
15. Y. D. Yu, Y. Cao, M. G. Li, G. Y. Wei and H. Dettinger, *Mater. Res. Innovations*, 18 (2014) 314.
16. G. V. Redkina, Y. I. Kuznetsov, N. P. Andreeva, I. A. Arkhipushkin and L. P. Kazansky, *Corros. Sci.*, 168 (2020) 108554.
17. Y. L. Wu, X. Y. Tan, Y. K. Wang, F. J. Tao, M. L. Yu and X. B. Chen, *Colloids Surf., A*, 634 (2022) 127919.
18. S. A. A. Kamal, R. Ritikos and S. A. Rahman, *Surf. Coat. Technol.*, 409 (2021) 126912.
19. Z. F. Lin, W. Zhang, W. Zhang, L. K. Xu, Y. P. Xue and W. H. Li, *Mater. Chem. Phys.*, 277 (2022) 125503.
20. Y. Y. Wang, M. P. Wu, P. P. Lu, W. Zhou, X. J. Shi, K. Yang and X. J. Miao, *Colloids Surf., A*, 632 (2022) 127824.
21. Y. D. Yu, G. Y. Wei, J. W. Lou, H. L. Ge, L. X. Sun and L. Z. Zhu, *Surf. Eng.*, 29 (2013) 234.
22. G. V. Redkina, Y. I. Kuznetsov, N. P. Andreeva, I. A. Arkhipushkin and L. P. Kazansky, *Corros.*

Sci., 168 (2020) 108554.
23. J. Chen, H. Y. Yang, G. Q, Xu, P. J. Zhang, J. Lv, W. Sun, B. S. Li, J. Huang, D. M. Wang, X. Shu and Y. C. Wu, *J. Rare Earths*, 17 (2020) 1.
24. S. Thomas, I. S. Cole, M. Sridhar and N. Birbilis, *Electrochim. Acta*, 97 (2013) 192.
25. A. J. Pan, R. R. Cai and L. Z. Zhang, *Appl. Surf. Sci.*, 568 (2021) 150872.
26. J. L. Song, W. J. Xu, X. Liu, Y. Lu, Z. F. Wei and L. B. Wu, *Chem. Eng. J.*, 211-212 (2012) 143.
27. G. Y. Li, X. P. Li, H. Wang, Z. Q. Yang, J. Y. Yao and G. F. Ding, *Microelectron. Eng.*, 95 (2012) 130.
28. D. Z. Liu, A. Z. Wang, G. Wang, K. X. Gui and M. Wang, *Mater. Des.*, 210 (2021) 110044.
29. X. S. Lv, Y. Qin, H. Liang, B. X. Zhao, Y. He and X. M. Cui, *Appl. Surf. Sci.*, 562 (2021) 150192.
30. J. B. Wang, M. Q. Cui, D. C. Wang, Y. Liu, J. Z. Cai, Z. Q. Gu and C. Q. Hu, *Ceram. Int.*, 47 (2021) 23653.
31. A. Rosales, L. Ortiz-Frade, I. E. Medina-Ramirez, L. A. Godinez and K. Esquivel, *Ultrason. Sonochem.*, 73 (2021) 105483.
32. K. B. Li, M. Li, C. Xu, Z. Y. Du, J. W. Chen, F. X. Zou, C. W. Zou, S. C. Xu and G. H. Li, *J. Mater. Sci. Technol.*, 88 (2021) 11.
33. M. Y. Zhang, E. Lei, R. R. Zhang and Z. F. Liu, *Surf. Interfaces*, 16 (2019) 194.
34. J. Y. Zheng, S. H. Bao and P. Jin, *Nano Energy*, 11 (2015) 136.
35. A. H. N. Nezhad, E. M. Zahrani and A. M. Alfantazi, *Corros. Sci.*, 197 (2022) 110095.
36. H. J. Yang, Y. M. Gao, W. C. Qin, J. P. Sun, Z. F. Huang, Y. F. Li, B. Li and J. L. Sun, *J. Alloys Compd.*, 898 (2022) 163038.
37. S. S. Xu, Q. Wang, N. Wang, L. Qu and Q. N. Song, *J. Cleaner Prod.*, 323 (2021) 129267.